

# A Transmit/Receive Active Antenna with Fast Low-Power Optical Switching

James Vian and Zoya Popović, *Senior Member, IEEE*

**Abstract**—This paper presents an optically switched X-band active antenna element for half-duplex transmit/receive (T/R) applications. The antenna element is designed to be a unit cell of a quasi-optical array with fast switching between T and R and with built-in phase-shifterless beamforming. The measured performance of the active element is 14 dB gain contributed by the power amplifier (PA) in transmission and 16 dB gain contributed by the low-noise amplifier in reception, with 30 dB isolation between T and R. The switching is accomplished with only 1  $\mu$ W of optical power for 1.7  $\mu$ s switching time (1.7 pJ of optical energy) and a rise time of 2 ns at 10 GHz with 7 mW of optical power (14 pJ of optical energy). The design, implementation, and measured performance of the optically controlled transmit/receive circuit are presented.

**Index Terms**—Active antennas, microwave switches, optical switches, switched circuits.

## I. INTRODUCTION

WITH THE increasing complexity of modern communication environments, antenna arrays with a number of simultaneous beams are of interest. One possible realization of multiple-beam arrays is active antenna array lenses (AAALs) with spatial feeds [1], [2]. Some properties of this architecture are phase-shifterless beamforming; lower feed losses than those associated with corporate feeds for a large number of array elements; improved dynamic range in reception; high effective isotropically related power in transmission; and graceful degradation in both transmit and receive modes [3], [4]. Transmit/receive (T/R) AAALs can operate in full-duplex or half-duplex modes. Full-duplex operation (simultaneous transmission and reception) requires separate array elements, selective duplexers (filters), or the use of circulators to route transmit and receive signals through the appropriate amplifiers. Half-duplex operation, the topic of this paper, uses microwave single-pole double-throw (SPDT) switches to route the transmitted and received signals.

Fig. 1 shows an example of a cylindrical active lens with half-duplex operation. Each array element contains two antennas (shown here as patch antennas on each side of the lens), a power amplifier (PA), a low-noise amplifier (LNA), and two SPDT switches. In transmission mode, the patch antennas on the feed side receive signals from one or more feed antennas (represented by horn antenna in the figure) located along the focal arc of the

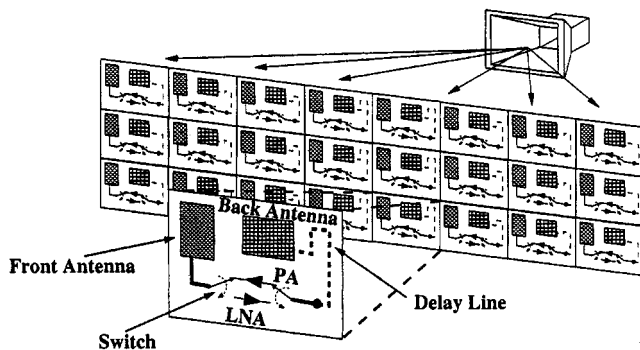


Fig. 1. Sketch of a cylindrical T/R active antenna lens array with half-duplex operation. The insert shows details of the array element (unit cell).

lens. In each element, the signal is delayed in relation to its position in the array: unit cells in the center have longer delays than edge elements, in analogy to an optical lens' being thicker in the center than on the edges. The switches then route the signals through PA's before retransmitting a coherent combination of all the element powers. In reception, the signals are routed through LNAs in each element. Different positions of a feed along the focal arc correspond to different main beam angles, since the lens is angle preserving. In addition, for linear amplifiers in the lens, several feeds can be used simultaneously for beamforming [5].

In half-duplex T/R lens arrays demonstrated to date, the switches are controlled in parallel and the bias and control lines contain capacitors that suppress bias-line oscillations [3], [4]. As a result, the rise and fall times of the array when it is switched between T and R increase with the number of array elements. Individual control of each element, however, increases the complexity of the control lines and the cost. A possible solution, discussed in this paper, is to optically control switches in each unit cell of an array [6]. In this case, the switching speed of the array is independent of its size and equal to the switching speed of each element. Further, optical fibers that guide the switching control signals do not affect the microwave fields.

Previously demonstrated optically controlled microwave switches use optical power to generate carriers in microwave p-i-n diodes [7]–[9]. The disadvantage to this technique is the fact that the insertion loss (IL) and isolation of the switch depend strongly on optical power, and as much as 40 mW of optical power can be required to achieve an IL of 1.2 dB and an isolation of 30 dB [9]. The optically controlled microwave switch presented in this paper uses a small amount of optical power to control the bias of chip p-i-n diodes. The advantage of this technique is that only the switching speed (rise and fall

Manuscript received March 1, 2000; revised August 25, 2000. This work was supported by the Office of Naval Research, by the Office of the Secretary of Defense under Multidisciplinary Research Initiative Program N00014-97-1-1006, and by the Army Research Office under Multidisciplinary Research Initiative Program DAAH04-98-1-0001.

The authors are with the Department of Electrical and Computer Engineering, University of Colorado, Boulder, CO 80309-0425 USA.

Publisher Item Identifier S 0018-9480(00)10747-1.

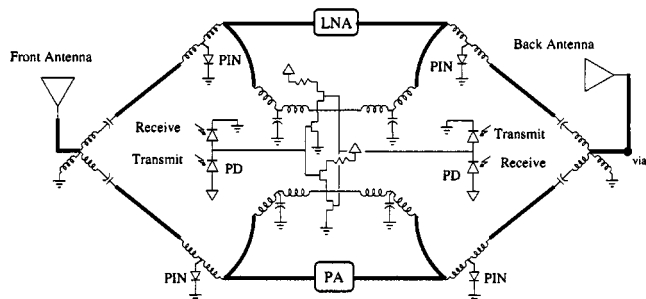


Fig. 2. Circuit diagram of the active antenna element. The light incident on the PDs controls the p-i-n diode SPDT switch through push-pull FETs. The switches route the signal between the two antennas: PA in transmission and LNA in reception.

times) is a function of incident optical power, while the IL and isolation are independent of it.

## II. DESIGN AND LAYOUT OF OPTICALLY CONTROLLED MICROWAVE T/R SWITCH

Fig. 2 shows the schematic of the array element used in this work. 10-GHz patch antennas with a common ground plane and vias between the two sides of the active antenna are used to improve isolation between the input and output of the amplifiers. Off-the-shelf monolithic microwave integrated circuit (MMIC) amplifiers are used for the PA<sup>1</sup> and LNA.<sup>2</sup> MA/Comm MA4GP032 p-i-n diodes, with a 3- $\Omega$  on-resistance at 3 mA and 0.12 pF capacitance in the off state, are used for the microwave switch. Diameter of 25  $\mu\text{m}$  and gold bond wires of length 0.5 mm are used as 1-nH inductors in a T-network with the p-i-n diodes to improve performance by reactance cancellation. The resulting single-pole single-throw (SPST) switch has a measured IL of 0.75 dB and an isolation of 20 dB from 6 to 13 GHz.

Compact high-pass filters (HPFs) and low-pass filters (LPFs) are needed to separate the bias/control and radio-frequency (RF) signals. In the unit cell, a second-order HPF isolates the bias control for each side of the SPDT switch. This filter exhibits at least 20 dB rejection below 1 GHz and 0.1 dB loss at 10 GHz. It is implemented with a 2-nH shunt bond wire and a 1-pF chip capacitor at 10 GHz (Fig. 3). An additional bond wire is needed to connect the chip capacitor to the microstrip line and is designed to be resonant with the capacitor at 10 GHz. A third-order LPF biases the p-i-n diodes implemented with 0.85-nH bond wires and 3-pF capacitors. The low impedance of this combination is transformed into a high impedance with a  $\lambda_g/4$ -long microstrip line causing a 0.1-dB transmission loss at the bias line junction and 33.9-dB bias line RF leakage (Fig. 4).

The optically controlled bias to the p-i-n diodes is implemented with a HP ATF26836 general purpose metal-semiconductor field-effect transistor (MESFET) (9 dB gain,  $f_T = 16$  GHz,  $C_{gs} = 2.2$  pF) and Fermionics FD80S3 1300-nm photodiodes (PDs) (0.95 A/W responsivity, active area 80  $\mu\text{m}$  diameter,  $C_j = 0.12$  pF). The MESFETs are used to sink and source the current of the p-i-n diodes, allowing for small on/off response

<sup>1</sup>HP HMMC-5618, 14 dB gain from 6 to 20 GHz with 18 dBm power at the 1-dB compression point.

<sup>2</sup>United Monolithic Semiconductor CHA2063, 16 dB gain from 8 to 13 GHz with a noise figure of 2 dB.

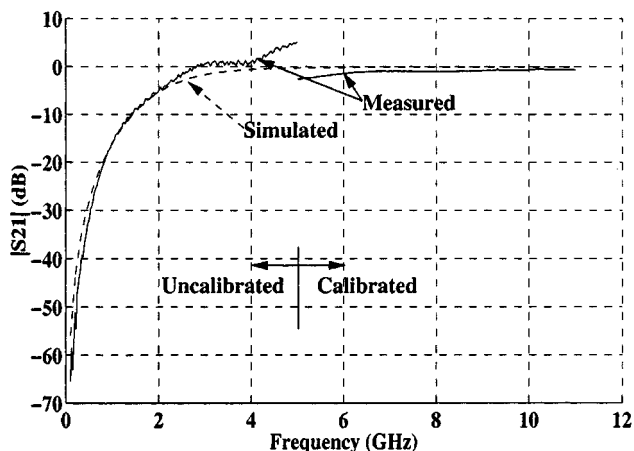


Fig. 3. Simulated (- -) and measured (-) high-pass filter transmission response. The filter consists of a chip capacitor and a shunt bond wire and is very compact.

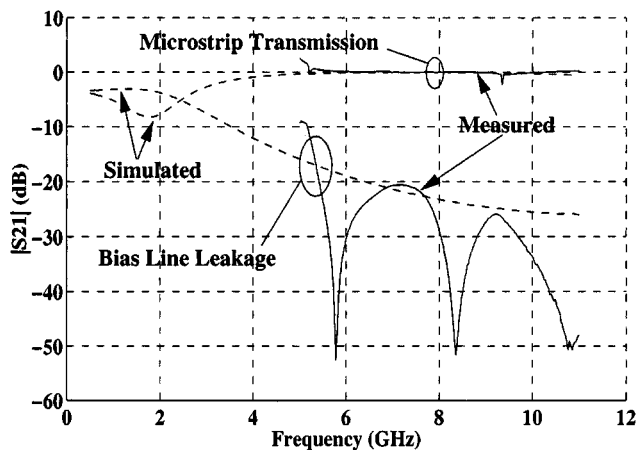


Fig. 4. Simulated (- -) and measured (-) p-i-n diode bias line transmission loss and RF leakage. This compact bias line is implemented with a chip capacitor, bond wire inductors, and single  $\lambda_g/4$  line section.

times. Push-pull PDs control the gate bias point for the MESFETs. The switch is supplied from the MMICs bias line through a current limiting resistor, eliminating the need for extra bias lines.

The MESFET gate capacitance and PD on-resistance dominate the rise and fall times of the bias control circuit. Fig. 5 shows SPICE simulation results for rise and fall time as a function of optical power per PD. The SPICE models for each component are based on physical measurements. It can be seen that the fastest expected response for the back-to-back SPDT switches is 2.4 ns at 9 mW per PD and is determined by the RC time constant resulting from the two p-i-n diode junction capacitance in parallel and the current-limiting resistor. Faster rise time may be achieved by reducing the impedance of the current limiting resistor at the cost of increased p-i-n diode current or providing a separate supply bias line for the switch. For only 1  $\mu\text{W}$  of incident optical power, the switch rise (and fall) time is approximately 1700 ns.

Fig. 6 shows the layout of the active antenna element. The active circuit side of the antenna element, Fig. 6(a), contains the two SPDT switches, LNA, PA, and patch antenna. The push-pull MESFETs and PDs are packed into the center of

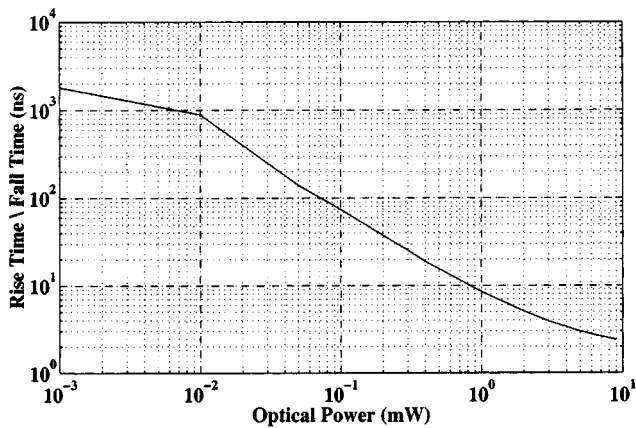
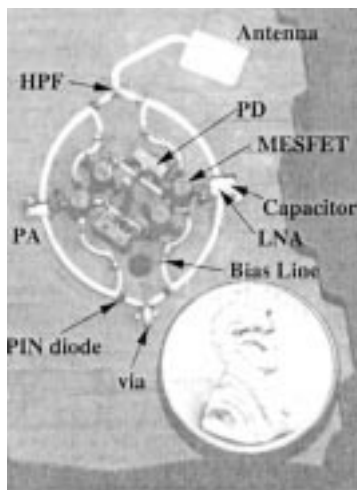
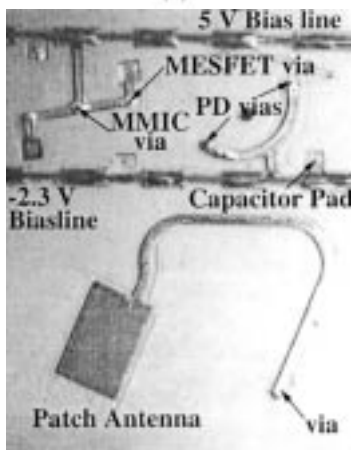


Fig. 5. SPICE simulation of rise and fall times of the optically controlled microwave switch as a function of optical power per photodiode.



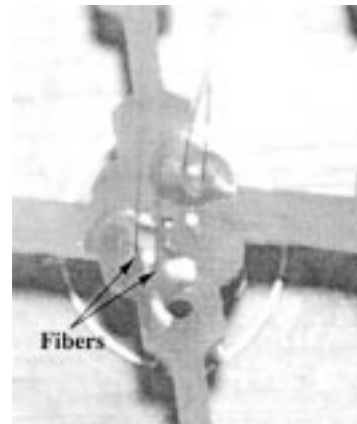
(a)



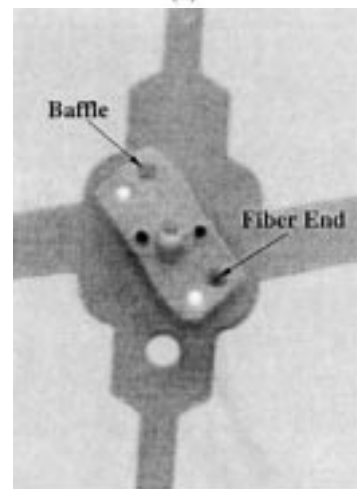
(b)

Fig. 6. Photographs of the antenna element without the fiber optic mount: (a) the active circuit side layout and (b) the passive side layout.

the circuit with the  $50\text{-}\Omega$  microstrip lines of SPDT switch encircling them. Isolation of 30 dB is maintained between any



(a)



(b)

Fig. 7. Photographs of optical fiber mount: (a) the top of the optical fibers mount and (b) the bottom of the optical fibers mount with the 1.5-mm baffle holes.

two elements that carry the 10-GHz signal in order to prevent oscillations.

The 5 V and  $-2.3$  V supply bias lines are on the passive side of the active antenna element [Fig. 6(b)]. The bias lines consist of sections of high and low impedance  $\lambda_g/4$  microstrip lines to prevent propagation of the 10-GHz signal. A 0.24-mm-diameter wire is soldered down the center of the bias line to reduce the dc impedance with a reduction of 0.5 dB in filtering performance at 10 GHz. The overall bias line suppression is  $-7.1$  dB/ $\lambda_g$ . The MMIC amplifiers from the 5-V supply bias line are decoupled by 100-pF chip capacitors on the active circuit side.

An optical mount shown in Fig. 7 aligns the optical fibers to the PD while protecting the circuit bond wires. Free space coupling from the fibers to the PDs allows access to the microwave circuit during testing. The optical mount uses five posts (one in the middle and four in each corner) to achieve a placement accuracy of  $40\text{ }\mu\text{m}$ . Unfortunately, the overall alignment of the fibers to the PDs is  $200\text{ }\mu\text{m}$ , limited by the packaging of the commercial PDs. The optical fiber is placed approximately 1 mm above the PDs, allowing natural diffraction of the light to cover the

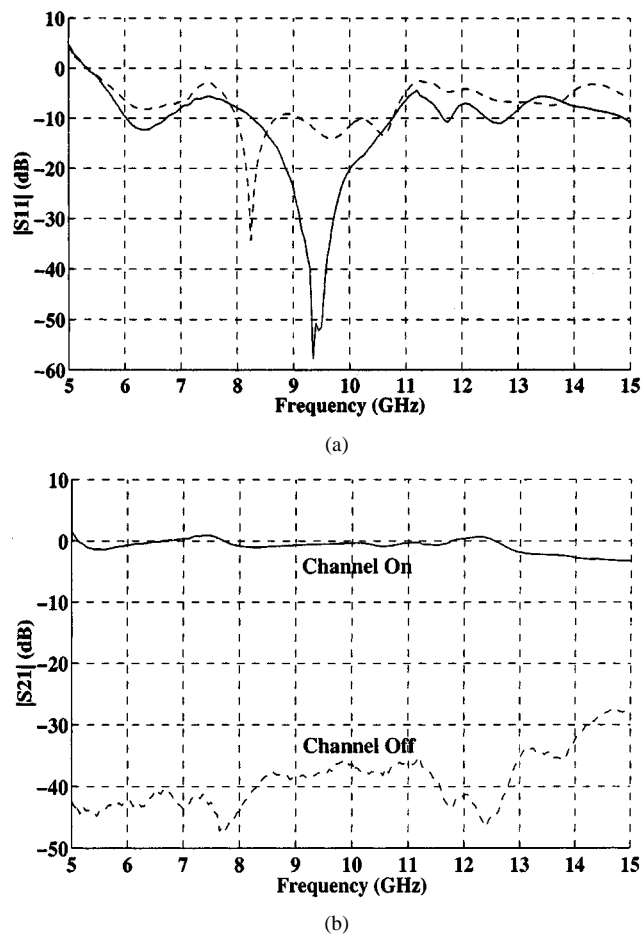


Fig. 8. Measured performance of the SPDT microwave switch: (a) return loss and (b) insertion loss and isolation.

area where the PD is mostly likely to be. This results in approximately 15.7 dB loss in optical power. The patch antenna radiates through a 20 mm by 20 mm aperture in the FR4 mount, which has measurable effects on the RF active antenna.

### III. PERFORMANCE OF THE OPTICALLY CONTROLLED SWITCH

The measured SPDT switch in the active antenna element has an IL of 0.31 dB and an isolation of 36 dB over a 2.5 GHz 2 : 1 voltage standing-wave ratio bandwidth (8.36 to 10.8 GHz) (Fig. 8). From the SPICE simulations, 90% of the spectral energy for the switching currents is below 700 MHz, allowing the removal of the shunt inductor in the HPF to improve the reflection loss. The series capacitor in HPF reduces the p-i-n diode switching voltage by 10 dB, which is sufficient to prevent the other p-i-n diode from turning on.

An optical power of 0.25  $\mu\text{W}$  per diode maintains the switch state. Therefore, the optical power from Fig. 5 is required only during the period of time in which the switch is changing state. Table I shows the required optical energies for changing state for different rise times of the switch.

For testing the optical switching rise and fall times, variable-length complementary optical pulses with fast edges are needed. Two 3-GHz uniphase intensity electrooptic (EO) modulators are used to generate the optical pulses. They are controlled by a function generator and inverting/noninverting op-amps and

TABLE I  
OPTICAL ENERGY NECESSARY FOR THE MICROWAVE SWITCH TO CHANGE STATE

Rise time (ns)	Optical Power (mW)	Energy (pJ)
2.4	9	21.0
3	5	15.0
8.5	1	8.5
25.4	0.3	7.6
140	0.05	7.0
888	0.01	8.9

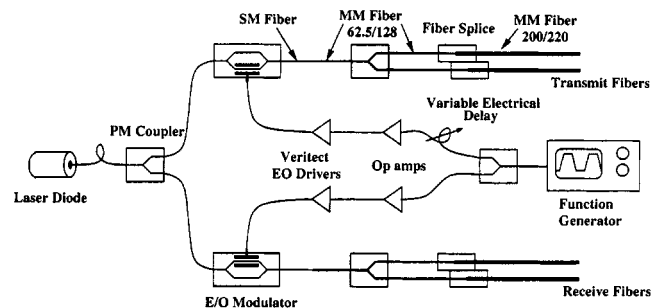


Fig. 9. Block diagram of test setup used to characterize the optical control circuit.

two Veritact EO drivers. An Ortel 10-mW 1300-nm fiber-pigtailed laser diode is the optical source, shown in Fig. 9. The resulting optical pulses are 25 to 7000 ns wide with constant rise (fall) time of about 1 ns, as represented in Fig. 10. The single-mode (SM) fiber outputs of the EO modulators are coupled to 62.5/128  $\mu\text{m}$  multimode (MM) fiber splitter, then spliced to 200/220  $\mu\text{m}$  fibers for easier free-space alignment to the PDs. Baffles [Fig. 7(b)] between the optical fibers and the PDs prevent cross-coupling between the transmit and receive optical control signals. The loss due to the free-space coupling of the fibers to the PDs limits the testing range of the switch from 3 to 15  $\mu\text{W}$  of optical power per diode, but this is not a fundamental limitation.

Two back-to-back optically controlled microwave switches were constructed to test the switch response of the active antenna element. In these measurements, an HP 83620 sweeper is connected in place of the patch antenna and an HP 54750 50-GHz oscilloscope in place of the MMIC amplifiers. The oscilloscope measures the change of the p-i-n diode bias; however, the bias circuitry is loaded, resulting in a slower response. The SPICE model was modified to include the effects of the oscilloscope, as well as the uncertainty in optical power delivered to the PDs (+1.7 dB and -2.7 dB).

Fig. 11 shows a comparison of the simulations with measurements, which fall within the modeled bounds. In the active antenna, the switching should be faster, since measurements of the MMICs using a network analyzer indicate a nearly perfect reflection (-0.6 dB) at each port for frequencies below 700 MHz.

### IV. PERFORMANCE OF ACTIVE T/R ANTENNA ELEMENT

The active T/R antenna was characterized with respect to an aperture of the same electrical size (0.75  $\lambda_0$  by 1  $\lambda_0$ ). First the aperture and then the active antenna are placed in a setup as

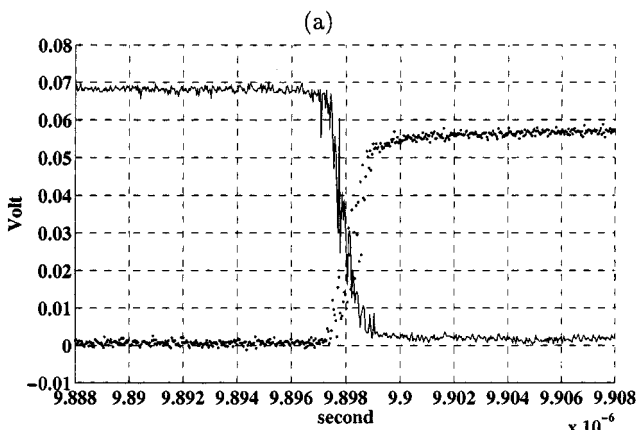
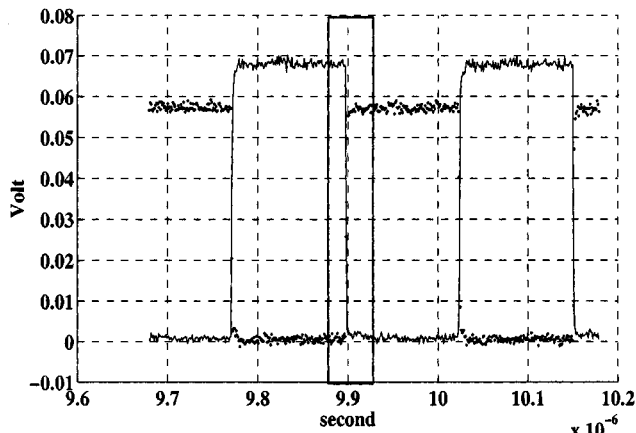


Fig. 10. Measured optical pulse at output of EO modulators. The rectangle indicated in (a) is expanded in time in (b) to show rise/fall times.

shown in Fig. 12(a). Two orthogonally polarized antennas are connected to the ports of a HP70820A transition analyzer. The aperture/active antenna is placed in the middle of the line-of-sight between them, and the antennas are placed in the far field. The gain over the power transmitted through the aperture is measured for the active antenna for both T and R paths with the amplifiers on and off. The gains of the PA and LNA are then estimated within a 2-dB accuracy from the active antenna gain and by using the Friis transmission formula. The loss due to aperture efficiency of the antennas is 4.7 dB from the ratio of the  $0.25 \lambda_0^2$  effective area of the patch antenna to the  $0.75 \lambda_0^2$  area of unit cell and ( $\sim 1$  dB) for 80% radiation efficiency. Other losses due to the via holes (1 dB) and the switch insertion loss (0.34 dB) are taken into account, yielding gains of 14 and 16 dB contributed by the PA and LNA, respectively. These gain levels are in agreement with the manufacturer's specifications for the MMICs. The gain in transmit and receive modes as a function of frequency is shown in Fig. 12(b), and the bandwidth is dictated by the patch antenna bandwidth, whereas the switch itself is broadband. The isolation is measured to be 30 dB or more for cases when the active antenna was in receive mode while transmitting, the active antenna was in transmit mode while receiving, and the active antenna was in the off state. These mea-

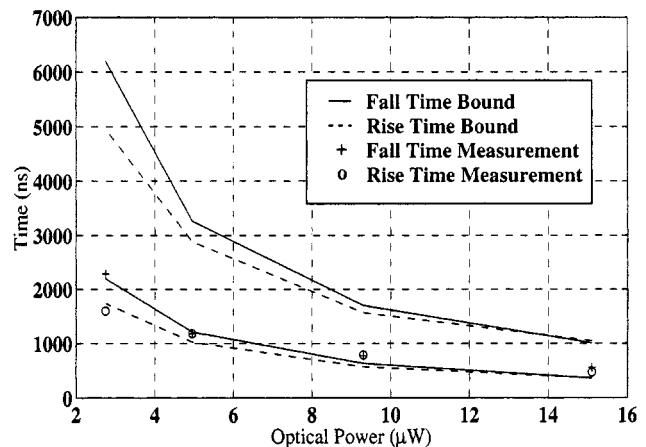


Fig. 11. Measured back-to-back SPDT switch rise time and fall time as a function of incident optical power.

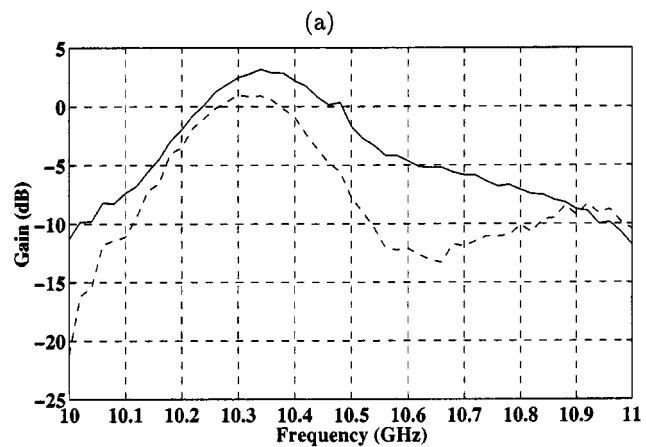
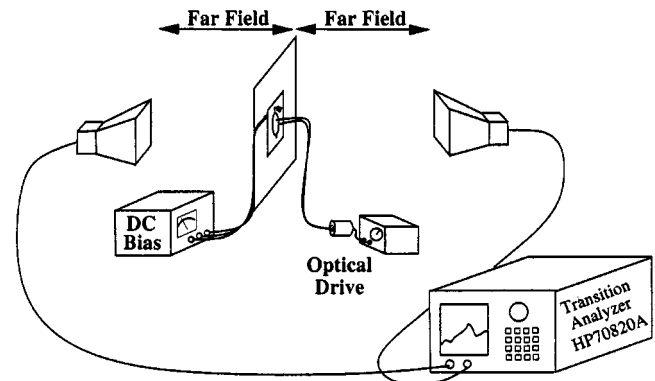


Fig. 12. Far-field characterization of the active antenna element: (a) the testing setup and (b) the measured gains of the active antenna as a function of frequency for receive mode (solid line) and transmit mode (dashed line).

surements are limited by edge diffraction and feed cross-polarization quality.

## V. DISCUSSION

In this paper, we describe the design and demonstration of a high-speed optically controlled T/R active antenna. This active

antenna is designed as an element of a  $6\lambda_0$  by  $3\lambda_0$  cylindrical active lens array with a focal-distance-to-diameter (F/D) ratio of one, a directivity of 20 dB, and a beamwidth of  $10^\circ$  in the focusing plane. The lens array implements beam switching and forming in both transmit and receive modes, and its performance, as applied to communication and radar systems, is currently being characterized.

The optically controlled SPDT switches used to route the signal in the active antenna have 0.31 dB insertion loss, 36 dB isolation, and  $-10$  dB return loss from 8.36 to 10.8 GHz. Unlike in previously demonstrated optically controlled microwave switches, these microwave parameters do not change with the amount of incident control (optical) power. However, the optical power level conveniently controls the switching speed alone, making the switch easily integrated into applications with different switching speed requirements. Microsecond switching required in most T/R applications can be accomplished with only microwatts of optical power, but some applications, such as phase shifters in phased array or polarization switching in multipath environments, could benefit from nanosecond switching speeds. Even though the 2.6-ns speed demonstrated in this paper requires relatively large optical power (about 10 mW), the optical energy is quite low: 21 pJ. For comparison, the fastest reported microelectrical mechanical system (MEMS) microwave switch has a rise time of about 1 to 5  $\mu$ s and requires about 2 nJ of control energy [10], [11]. The switch presented here draws more electrical power (3 mA per p-i-n diode) than a MEMS switch, but the required dc current is a small fraction of the 160 mA drawn by the LNA and PA. However, the optically controlled microwave switch requires significantly less control energy than a MEMS switch, since the energy distribution is fundamentally different. In some respects, it is easier to generate fast optical pulses than to generate fast high-voltage (30–50 V) electrical pulses.

The active array element is designed with off-the-shelf components not optimized for speed or low power, and the coupling of light from the fibers is not optimal. Therefore, the presented results are by no means fundamentally limited, and we expect that significant improvements can be made by using PDs with better placement tolerances, using chip MESFETs for the p-i-n diode bias control, and by improving the coupling efficiency of the light into the PD (using, e.g., microlenses and printed optical waveguide structures). Ultimately, a large portion of the switch, and in principle the entire switch circuit, can be implemented monolithically.

#### ACKNOWLEDGMENT

The authors thank G. Kriehn at the University of Colorado for helpful discussions.

#### REFERENCES

- [1] W. Rotman and R. F. Turner, "Wide-angle microwave lens for line source applications," *IEEE Trans. Antennas Propagat.*, vol. 11, pp. 623–632, Nov. 1963.
- [2] D. T. McGrath, "Planar three-dimensional constrained lens," *IEEE Transactions on Antenna and Propagation*, vol. 34, Jan. 1986.
- [3] Z. Popović, "Quasioptical transmit/receive front ends," *IEEE Trans. Microwave Theory Tech.*, vol. 48, pp. 1964–1975, Nov. 1998.
- [4] S. Hollung, A. Cox, and Z. Popović, "A bi-directional quasioptical lens amplifier," *IEEE Trans. Microwave Theory Tech.*, vol. 45, pp. 2352–2357, Dec. 1997.
- [5] J. S. H. Schoenberg, S. C. Bundy, and Z. B. Popović, "Two-level power combining using a lens amplifier," *IEEE Trans. Microwave Theory Tech.*, vol. 42, pp. 2480–2485, Dec. 1994.
- [6] J. Vian, P. Kirkpatrick, and Z. Popović, "An optically controlled transmit/receive active antenna," in *Proc. DARPA Symp. Photonic Systems for Antenna Applications*, vol. 9, Feb. 1999.
- [7] P. J. Stabile, A. Rosen, and P. R. Herczfeld, "Optically controlled lateral p-i-n diodes and microwave control circuits," *RCA Rev.*, pp. 443–456, Dec. 1986.
- [8] J. L. Freeman, S. Ray, D. L. West, A. G. Thompson, and M. J. LaGasse, "Microwave control using a high-gain bias-free optoelectronic switch," *Proc. SPIE Optical Technology for Microwave Applications*, vol. 5, pp. 320–325, 1991.
- [9] S. S. Gevorgian, "Short-circuit photocurrent-controlled microwave p-i-n diode switch," *Microwave Opt. Technol. Lett.*, vol. 7, no. 12, pp. 553–555, Aug. 1994.
- [10] C. L. Goldsmith, Z. Yao, S. Eshelman, and D. Denniston, "Performance of low-loss RF MEMS capacitive switches," *IEEE Microwave Guided Wave Lett.*, vol. 8, pp. 269–271, Aug. 1998.
- [11] E. R. Brown, "RF-MEMS switches for reconfigurable integrated circuits," *IEEE Trans. Microwave Theory Tech.*, vol. 46, pp. 1868–1880, Nov. 1998.

**James Vian**, photograph and biography not available at the time of publication.

**Zoya Popović** (S'86–M'90–SM'99) received the Dipl. Ing. degree from the University of Belgrade, Serbia, Yugoslavia, in 1985, and the M.S. and Ph.D. degrees from the California Institute of Technology, Pasadena, in 1986 and 1990, respectively.

She is currently an Associate Professor of electrical and computer engineering at the University of Colorado at Boulder. Her research interests include microwave and millimeter-wave quasi-optical techniques and active antenna arrays, high-efficiency microwave circuits, RF photonics, and antennas and receivers for radioastronomy.

Dr. Popović was the recipient of the 1993 URSI Young Investigator Award and the 1993 National Science Foundation Presidential Faculty Fellow Award, and the 1996 URSI International Issac Koga Gold Medal. She was also the recipient of the 1993 IEEE Microwave Theory and Techniques Society (IEEE MTT-S) Microwave Prize for pioneering work in quasi-optical grid oscillators.